https://doi.org/10.5194/bg-2022-91
Preprint. Discussion started: 13 April 2022

Biogeosciences
Discussions
Open Access

Acidification impacts and acclimation potential of foraminifera

Daniel François[1,4]*, Adina Paytan[2], Olga Maria Oliveira de Araújo[3], Ricardo Tadeu Lopes[3], Cátia Fernandes Barbosa[1]

[1]Departamento de Geoquímica, Universidade Federal Fluminense, Niterói, Brazil.
[2]Institute of Marine Sciences – University of California, Santa Cruz, USA.
[3]Federal University of Rio de Janeiro (UFRJ), Nuclear Instrumentation Laboratory, Nuclear Engineering Program/COPPE, Rio de Janeiro, Brazil
[4]Department of Ocean Systems, NIOZ Royal Netherlands Institute for Sea Research and Utrecht University, Texel, the Netherlands

*Correspondence author: danielfrancois@id.uff.br

Abstract. Ocean acidification is expected to negatively affect many ecologically important organisms. Here we explored the response of Caribbean benthic foraminiferal communities to naturally discharging low-pH waters similar to expected future projections for the end of the 21st century. At low-pH (~ 7.7 pH units), low calcite saturation, agglutinated and symbiont-bearing species were relatively more abundant, indicating higher resistance to potential carbonate chemistry changes. Diversity and other taxonomical metrics declined steeply with decreasing pH despite exposure of this ecosystem for millennia to low pH conditions, suggesting that tropical foraminifera communities will be negatively impacted under acidification scenarios SSP3-7.0 and SSP5-8.5. The species *Archaias angulatus*, a major contributor to sediment production in the Caribbean was able to calcify at conditions more extreme than those projected for the late 21st century (7.1 pH units), but the calcified tests were of lower density than those exposed to high-pH ambient conditions (7.96 pH units), indicating that reef foraminiferal carbonate budget might decrease. Smaller foraminifera were highly sensitive to decreasing pH and our results demonstrate their potential as indicators to monitor increasing OA conditions.

1 Introduction

With anthropogenic carbon emissions steadily increasing since the beginning of the industrial age, atmospheric carbon dioxide (CO_2) is now higher than it has been in the past 800 thousand years (Petit et al., 1999; Lüthi et al., 2008). Global emissions are annually increasing and leading a proportional increase of CO_2 uptake by the oceans and consequently decrease of surface ocean pH (-0.0181 ± 0.0001 decade^{-1}, Lida et al., 2021) and carbonate ion concentrations [CO_3^{2-}], a process known as ocean acidification (OA) (Doney et al., 2020). Following the results of the Coupled Model Intercomparison Project Phase Six (CMIP6), a further decrease of surface ocean pH is expected for all Shared Socioeconomic Pathways (SSPs) at the end of the 21st century (Kwiatkowski et al., 2020; IPCC, 2021). As the carbonate system has major control on biogenic calcification efficiency this process is expected to negatively affect many ecologically important calcifying organisms such as corals (Kroeker et al., 2013; Hughes et al., 2017), foraminifers (Uthicke, Momigliano, and Fabricius, 2013; Kawahata et al., 2019), and coralline crustose algae (Penã et al., 2021).

Among these, foraminifera are dominant members of benthic communities with widespread distribution in the oceans. During their lifespan, they are vital to $CaCO_3$ cycling, especially through calcification (Langer et al., 1997; Langer, 2008). On a global scale, they are estimated to contribute a total of 14 billion tons of calcium carbonate per year, which accounts for about 25 % of current total calcium carbonate production (Langer, 2008). Due to their ability to consume substantial amounts of organic matter, they are also relevant for organic carbon cycling (Moodley et al., 2000), being part of a key link in marine food chains. After death, their tests became important contributors to sediment mass accumulation in many ecosystems (Yamano, Miyajima, and Koike, 2000; Doo et al., 2016) and are also relevant for the carbon burial flux in the ocean (Schiebel, 2002). With ongoing OA and future scenarios projecting rapid changes (Kwiatkowski et al., 2020; IPCC, 2021), it is vital to understand how foraminifera will be affected for assessing biological feedbacks and changes in biochemical cycles. To date, many studies under controlled conditions often document the association of low-pH with decreased calcification, weight, size, and taxonomical metrics (Nehrke et al., 2013; Kawahata et al., 2019; Narayan et al., 2021, and references therein). However, some studies have also demonstrated either resilience (Engel et al., 2015; Pettit et al., 2015; Stuhr et al., 2021), or even positive effects on foraminifera, such as enhanced calcification (Fujita et al., 2011) and enzymatic calcification activity (Prazeres et al., 2015), which demonstrate the complexity of interspecific responses to OA. Additionally, relatively little is known about how foraminifera respond in natural low-pH low carbonate saturation waters, which is crucial for determining if and how communities have the potential to acclimate.

In situ investigations have been performed in natural CO_2 vents in the Mediterranean Sea (Dias et al., 2010; Pettit et al., 2015), Papua New Guinea (Uthicke, Momigliano, and Fabricius, 2013), the northern Gulf of California (Pettit et al., 2013) and coastal springs in Puerto Morelos (PM), Mexico (Martinez et al., 2018). In the latter, recruitment and early succession (Crook et al., 2016), acclimatization potential (Crook et al., 2013), and the responses of calcifying communities were studied (Crook et al., 2012; Martinez et al., 2018), notably demonstrating that despite general deleterious effects some calcifiers were relatively resilient to OA. Specifically, a study focused on Large Benthic Foraminifera (LBF) has shown that porcelaneous, chlorophyte-bearing foraminifera, (e.g., *Archaias angulatus*), were relatively less impacted (Martinez et al., 2018). Study sites such as coastal springs allow the investigation of foraminiferal communities under projected future conditions more realistically, helping to decrease the uncertainty in global-scale models. However, a detailed survey considering community-wide responses (i.e., including smaller foraminifera) is necessary to ascertain a wider range of potential impacts.

As CO_2 emissions continue to grow despite emerging climate policies (Peters et al., 2020), global awareness has demonstrated a strong interest in research focused on potential impacts for mitigative action. To build on and expand the findings at PM we aimed to (i) investigate the effects of OA on both large and small foraminiferal assemblages for acidification scenarios projected to the end of the 21st century (Kwiatkowski et al., 2020; IPCC, 2021), (ii) explore the taphonomical and ecological implications of *postmortem* alterations for reef ecosystems, and (iii) investigate possible acclimation patterns in the shell structure of the species *Ar. angulatus*. Specifically, an examination of assemblage structure, taxonomic metrics, assemblage test size, preservation potential and an X-ray micro-CT analysis in the species *Ar. angulatus* was employed.

2 Methods

2.1 Study site and data retrieval

The Yucatán Peninsula is a karstic region in Southern Mexico (Fig. 1a). The geology is dominated by Tertiary limestones underlain by an ejecta/evaporite complex, where several structural and tectonic features strongly influence and divide the area into six distinct physiographic regions (Back and Hanshaw, 1970). Among these, Puerto Morelos reef lagoon is part of the Holbox Fracture Zone–Xel-Ha region, which is characterized by >100 km long chain of elongated depressions referred as 'sabanas' (Perry, Velazquez-Oliman, and Marin, 2002). In this area, rainwater infiltrates the porous karstic limestone of Quintana Roo (Fig. 1b) and flows towards the ocean through interconnected caves and fractures where the groundwater mixes with seawater in the underground aquifers before discharging between the shore and the offshore barrier reef (Beddows et al., 2007; Null et al., 2014). Flowing through the limestones and interacting with the strata through processes of dissolution, precipitation, and mixing, the groundwater conditions change and finally discharge along the Mexican coast as low-pH, low carbonate-saturation-state (Ω), and high inorganic C content waters (Back and Hanshaw, 1970; Perry, Velazquez-Oliman, and Marin, 2002; Crook et al., 2012, 2013, 2016; Martinez et al., 2018, 2019). These waters discharge at submarine springs, which structure ranges from long ''fractures'' to small circular depressions "seeps" (Fig. 1d, spring Agua), (Crook et al., 2012). The discharge of the springs is relatively constant throughout the year (Crook et al., 2016).

Surface sediment samples (~ 1 cm depth, coarse sand) were retrieved using a spoon at various distances from the center of six submarine springs (Fig. 1c, Gorgos, Laja, Mini, Norte, Agua, and Pargos) in October 2011. In the laboratory, samples were weighed, washed with deionized water through a 63 µm sieve mesh, and dried at 50 °C for 24 hours. Discrete water samples near the site of sediment collection were also retrieved for water chemical analysis. Water samples were filtered (0.2 µm) and split into aliquots for the analysis of salinity, total inorganic carbon (C_T) and total alkalinity (A_T), following the protocols of Dickson, Sabine and Christian (2007). The C_T was measured on a CM5011 Carbon Coulometer (UIC, Inc.; analytical measurement error: ± 3 µmol kg^{-1}) and T_A using an automated open-cell, potentiometric titrator (Orion model 950; analytical measurement error: ± 2 µmol kg^{-1}). Salinity was measured using a portable salinometer (Portasal Model 8410, Guild Line). Seawater temperature was measured in situ with a handheld YSI analyzer (Yellow Springs model 63). Water pH, carbonate ion concentration (CO_3^{2-})and calcite saturation state (Ω-Calcite) were calculated using the program CO_2Sys (Pierrot, Levis and Wallace, 2006), considering the CO_2 dissociation constants of Lueker, Dickson and Keeling (2000); $KHSO_4$ – Dickson, Sabine and Christian (2007); B concentration – Uppström, 1974. Certified CO_2 reference material (from A. Dickson lab at UC San Diego, batch 112) was used to calibrate all instruments.

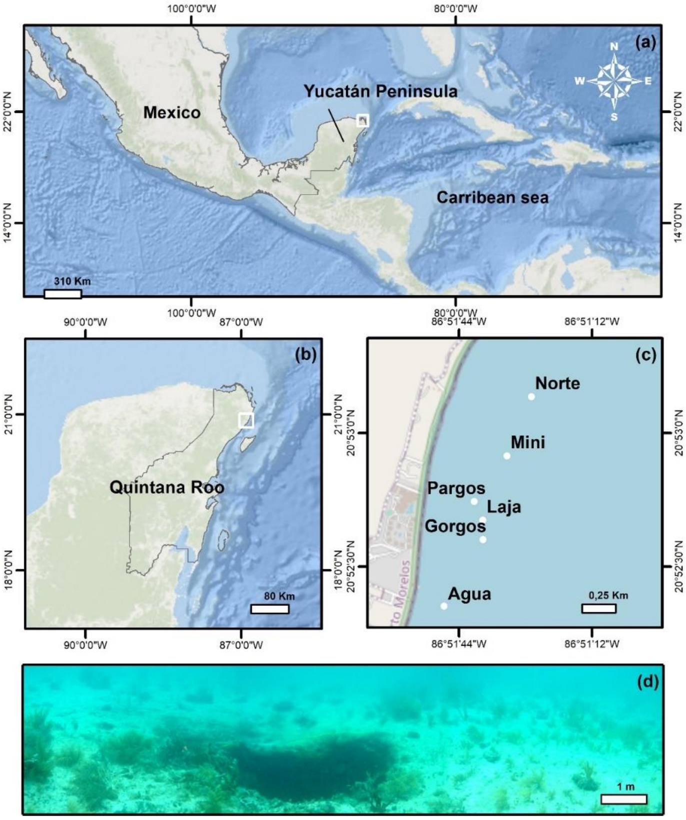

Figure 1 (a) Location map of the Yucatán Peninsula, (b) Quintana Roo, and (c) the six submarine springs (Gorgos, Laja, Mini, Norte, Pargos and Agua) studied at Puerto Morelos reef Lagoon (National Marine Park), (d) Spring agua, which structure presents a small circular depression.

2.2 Foraminiferal analysis

The dry weight of sediments was recorded, and samples were split to make them more suitable and efficient to pick. The specimens found in each pre weighted sediment aliquot were counted under a Zeiss STEMI 2000 stereomicroscope until a minimum of 250 specimens were obtained from each sample. Foraminiferal tests were identified to the lowest possible taxonomic level and assigned to informal species categories for diversity analyses. The taxonomic classification was based on the specialized bibliography of Cushman (1929), Jones (1994), and supplementary taxonomic studies (Milker and Schmiedl, 2012; Abu-Zied, Al-Dubai, and Bantan, 2016; Sariaslan and Langer, 2021). Each species and genus were verified against WoRMS to ensure the use of the most recent nomenclature.

The samples were stained in rose Bengal to consider the living counts in faunal analysis. Specimens were considered "alive" when all chambers, except for the last one or two, were well stained. Non-transparent agglutinated and miliolid taxa were broken to inspect their contents. Proportions of stained specimens were small (~3 %) and hence total (live plus dead) assemblages were used. The low live percentage is a common pattern as most reef-dwelling taxa tend to live on phytal or hard substrates rather than directly on the sediments (Martin, 1986; Barbosa et al., 2009, 2012; Stephenson, Hallock and Kelmo, 2015). Shannon-Weiner Diversity Index (H′), and Pielou's evenness (J′) were calculated considering the standardized foraminifera density at 1 ml. These taxonomic metrics were calculated as follows: Shannon-Weiner Diversity Index with the equation $H'=-\Sigma(Pi*\log(Pi))$, where Pi is the proportion of individuals per species; Pielou's evenness with the equation $J'=H'/\log(S)$, where H′ is the Shannon-Weiner Diversity Index and S the species richness. Assemblage distributions were also assessed according to differences in functional groups, i.e., symbiont-bearing and opportunistic, and test type groups, i.e., small miliolids, small rotaliids, and agglutinated that do not present an opportunistic behavior. This approach is used by Amergian et al. (2022) in nearby settings, based on categories designed by Hallock et al. (2003) for sensitivity/stress-tolerance taxa and Murray (2006) for different test compositions.

2.3 Taphonomy and assemblage test size analysis

To improve the understanding of the extent to which tests have been taphonomically altered a quantitative taphonomical analysis was conducted using a light microscope considering larger-scale structural damage such as breakage and dissolution. In the latter, any sign of dissolution, even if minimal, was considered. For a complete survey of the assemblage test size distribution, the surface area of all individuals was calculated using the ImageJ software (Schneider, Rasband, and Eliceiri, 2012). All specimens picked were placed on the dorsal side in common brass picking trays and photographed under the same magnification and camera settings using an adapter for a microscope camera. A similar procedure was performed by Prazeres et al. (2015) to trace surface area changes (i.e., gain or loss) in large benthic foraminiferal species under low-pH conditions. The parameter of surface area was the most suitable for the analysis since it identifies the size of the foraminifera tests in a standard way, considering the high taxonomical and consequently morphological diversity of PM samples.

2.4 X-ray MicroCT

An X-ray MicroCT analysis was employed in four individuals from high (7.96 pH units) and low-pH conditions (7.11 pH units). To ensure that the analyzed tests represent living conditions, only tests in excellent condition, and therefore, not influenced by post-mortem processes of dissolution and transport were selected. For the X-ray microCT acquisition, a V/TOMEX/M (GE Measurement and Control Solutions, Wunstorf, Germany) was used. The microCT parameters for the acquisition included a voltage of 60 kV, current of 100 µA, 5 frames, and an Al filter with a thickness of 0.5 mm. The geometry had a magnification of 31.81, pixel size of 6.28 µm. Certified calcite standards were used to calibrate the density for this material. The 3D reconstructions were performed using the Phoenix Datos X Reconstruction software, in which the slice alignment, beam hardening correction was implemented, and a mathematical edge-enhancement filter was applied to achieve a higher contrast between the edges. For the 3D visualization, VG Studio Max v 3.0 and Avizo 2020.3 softwares were used. For calcite density analysis,

https://doi.org/10.5194/bg-2022-91
Preprint. Discussion started: 13 April 2022

the CTAnalyser v. 1.18.4.0 software was used. Calcite density was assessed by the calcite density distribution calculated from the CT number that was calculated based on the X-ray attenuation coefficient of each sample. In addition, the estimation of morphometric parameters such as total volume and chamber wall thickness distribution was performed.

2.5 Statistical analysis

Cluster analysis of group average was performed using a similarity matrix (Bray-Curtis) of square-root-transformed abundances of foraminifera (≥3 %) with a second permutation procedure, the similarity profile (SIMPROF) routine (Clarke and Gorley, 2006). The matrix was also used to perform the similarity percentages analysis (SIMPER) to define which species contributed most to the forming groups considering a 90 % cut. Non-metric multidimensional scaling (nMDS) was used to visualize the similarity in foraminiferal assemblages. A BIO-ENV procedure (9999 permutations) and global BEST test (statistical significance) was used to identify the set of explanatory environmental parameters that produced a Euclidean matrix that best correlated (Spearman method) the species assemblage similarity matrix and normalized environmental variables. A Canonical Correspondence Analysis (CCA) was also used to explore the relationship between the biological and water chemistry data. Data normality and variance homogeneity were tested using Shapiro-Wilk and Levene's Test. For comparison of *Ar. angulatus* microstructure parameters between high and low-pH the student's t-test was used for variables with normal distributions and homogenous variances. When these conditions were not met, Welch's t-test was performed. We used the Kruskal-Wallis test to assess differences between functional groups, taxonomic metrics, and assemblage test size. The stations were separated into four groups considering the following pH gradients in respect to future projections: 8.1-8.05 pH units as present-day conditions; 8-7.9 pH units surveying low-intermediate acidification scenarios SSP1-2.6 and SSP2-4.5; 7.8-7.7 surveying high acidification scenarios SSP3-7.0 and SSP5-8.5; 7.6-7.2 surveying acidification conditions beyond those predicted to the end of 21st century. SIMPER, SIMPROF, nMDS, and BIO-ENV procedure were performed in Primer v.6 software (Clarke and Gorley, 2006). Student's t-test, Welch's t-test, Kruskal-Wallis test, and data visualization were performed using R software (version 4.0.2; http://www.Rproject.org, R core team, 2020). The CCA analysis was performed in PAlaeontological STatistics-PAST software (version 4.09).

3 Results

3.1 Water chemistry

Seawater carbonate chemistry (Table 1) contrasted strongly between samples. Obtained ranges were as follows: pH = 7.2–8.1 units, Ω-Calcite = 1.3–6.2, CO_3^{2-} = 52–240 µmol/kg^{-1}, T_A = 2044-3108 µmol/kg^{-1}, and C_T = 1725–3197 µmol/kg^{-1}. The temperature was consistent in ranging from 26.1–27.9 while salinity decreased with proximity to the springs, ranging from 28–37. As described in previous studies conducted at the same sites the salinity at the springs is > 30 over 90 % of the time and does not drop below 27 (Crook et al., 2012), and therefore is expected to produce little to no effect on foraminiferal communities (Martinez et al., 2018). The BIOENV analysis and global BEST test revealed that the best combination (p-value = 0.01) of environmental variables with species abundance was observed when considering pH, CO_3^{2-}, Ω

Calcite and T (ρ = 0.55), in which CO_3^{2-} and pH were the environmental variables matching the highest correlation (ρ = 0.5) and temperature the lowest (ρ = 0.038).

Table 1 Carbonate chemistry parameters of discrete water samples collected near the substrate at the time of sediment collection. T_A = total alkalinity; C_T = total inorganic carbon; CO_3^{2-} = carbonate ion concentration; Ω Calcite = calcite saturation-state; T = temperature. 205

Site	Depth (m)	Sample ID	A_T (µmol/kg^{-1})	C_T (µmol/kg^{-1})	pH	CO_3^{2-} µmol/kg^{-1})	Ω Calcite	T (C°)	Salinity
Norte	5.8	1	2611	2588	7.38	67.03	1.66	27.5	32.21
		2	2734	2734	7.34	60.93	1.53	27.2	30.70
		3	2699	2694	7.34	62.20	1.54	27.2	31.90
		4	2451	2314	7.66	118.47	2.85	27.0	35.25
Pargos	6.8	6	3000	3048	7.23	52.73	1.33	27.6	29.95
		7	3054	3047	7.38	71.16	1.82	27.7	28.00
		8	2304	2160	7.72	119.78	2.97	27.6	32.00
		9	2387	2084	8.00	220.39	5.36	27.5	34.20
		10	2336	2012	8.01	229.56	5.49	27.6	36.17
Gorgos	7.2	12	2350	2065	7.98	207.09	5.03	27.3	34.40
		13	2364	2004	8.10	255.79	6.18	26.8	34.80
		14	2044	1725	8.09	21608	5.24	26.9	34.40
		15	2325	2033	7.96	209.44	5.02	27.8	35.90
Laja	5.8	16	2827	2756	7.51	102.65	2.50	27.9	32.75
		17	2590	2385	7.83	164.17	4.00	26.1	33.70
		18	2354	2013	8.05	240.04	5.70	26.4	36.70
		19	2319	2051	7.94	192.93	4.59	26.5	36.60
		20	2357	2092	7.90	193.55	4.63	28.1	36.17
Agua	5.4	21	2444	2167	7.93	203.84	4.90	27.4	35.60
		22	2364	2128	7.87	176.51	4.27	28.0	35.10
		23	2314	2088	7.85	168.22	4.07	28.4	35.10
		24	2347	2063	7.95	206.13	4.98	28.2	35.10
		25	2363	2049	8.01	226.08	5.47	27.7	34.90
Mini	4.9	44	2443	2071	8.08	265.01	6.31	26.9	36.50
		45	2365	2113	7.90	184.16	4.37	26.6	36.90
		46	2356	2049	7.99	218.13	5.16	26.4	37.30

3.2 Foraminiferal analysis

The assemblages found at PM exhibit similar composition to previous studies conducted in nearby coastal settings (Gischler and Möder, 2009), Caribbean eastern islands (Wilson and Wilson, 2011), and the Gulf of Mexico (Stephenson, Hallock and Kelmo, 2015; Amergian et al., 2022). A total of 8564 foraminifera from 141 species were identified, belonging to 4 orders, 37 families, and 73 genera (Table S1). Agglutinated species contributed ~ 6.4 % (9 species), porcelaneous 61 % (86 species), and hyaline 32.6 % (45 species) of the total species richness. The species *Ar. angulatus* (9.4 %), followed by *Rotorbinella rosea* (9.3 %), *Asterigerina carinata* (6.9 %), and the *Rotorbis auberii* (4.7 %) were the most important contributing taxa. Considering a 3 % contribution cutoff a total of 34 species were considered for the faunal analysis (Fig. 2).

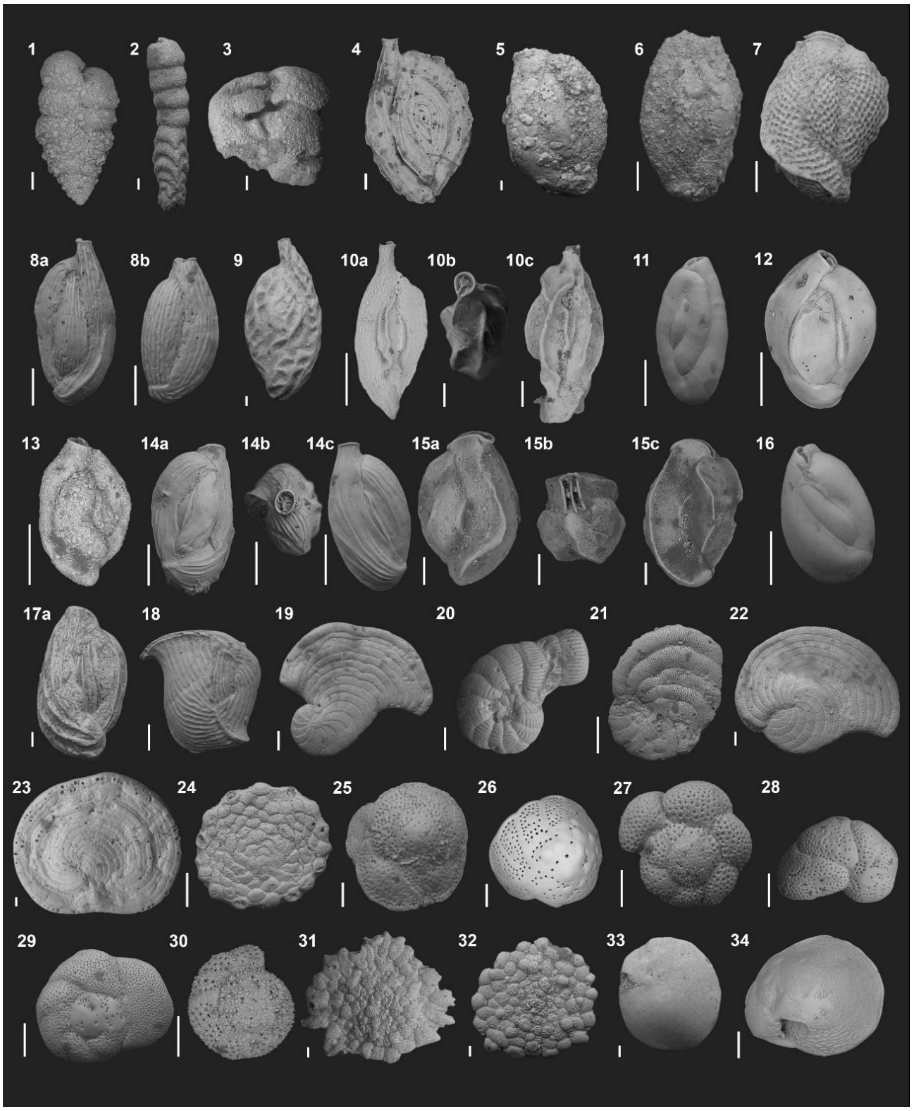

Figure 2 Electron micrographs of the species from Puerto Morelos reef lagoon springs considered for faunal analysis. Legend: ***1*** *Textularia agglutinans*, lateral view. **2** *Clavulina angularis*, lateral view. **3** *Valvulina oviedoiana*, lateral view. **4** *Spiroloculina corrugata*, lateral view. **5** *Agglutinella compressa*, lateral view. **6** *Schlumbergerina alveoliniformis*, lateral view. **7** *Lachlanella carinata*, lateral view. **8** *Quinqueloculina subpoeyana*, lateral view. **9** *Quinqueloculina tricarinata*, lateral view. **10a, 10c** *Quinqueloculina* conf. *Quinqueloculina distorqueata*, lateral views. **10b** *Quinqueloculina* conf. *Quinqueloculina distorqueata*, apertural view. **11** *Quinqueloculina bosciana*, lateral view. **12** *Quinqueloculina disparilis*, lateral view. **13** *Quinqueloculina* conf. Q. *berthelotiana*, lateral view. **14a,14c** *Quinqueloculina carinatastriata*, lateral views. **14b** *Quinqueloculina carinatastriata*, apertural view. **15a,15c** *Affinetrina quadrilateralis*, apertural views. **15b** *Affinetrina quadrilateralis*, apertural view. **16** *Miliolinella elongata*, lateral view. **17** *Pseudotriloculina linneiana*, lateral view. **18** *Articulina pacifica*, lateral view. **19** *Laevipeneroplis proteus*, lateral view. **20** *Peneroplis pertustus*, lateral view. **21** *Peneroplis planatus*, lateral view. **22** *Archaias angulatus*, lateral view. **23** *Cyclorbiculina compressa*, lateral view. **24** *Sorites marginalis*, lateral view. **25** *Rotorbis auberii*, spiral view. **26** *Rotorbinella rosea*, spiral view. **27** *Trochulina* sp, spiral view. **28** *Rosalina* cf. *floridana*, spiral view. **29** *Rosalina globularis*, spiral view. **30** *Cibicidoides* sp, spiral view. **31** *Planorbulina mediterranensis*, lateral view. **32** *Planogypsina acervalis*, lateral view. **33** *Amphistegina gibbosa*, lateral view. **34** *Asterigerina carinata*, lateral view. Scale bar represents 100 µm.

The relationship between water chemistry and species abundance can be visualized in the CCA diagram (Fig. 3), where a gradient of acidification stress is represented by Axis 1 (p-value = 0.001), which explains roughly 63 % of the total variance. In CCA, the environmental variables are represented by vectors, and their length reflects the relative importance to species distribution. As observed in BIOENV and global BEST analysis, CCA indicates that pH represents the most important variable to foraminifera distribution, while the temperature is the least. Species at the left side of Fig. 3 (e.g., *Quinqueloculina tricarinata*, *Ar. angulatus*, *Amphistegina gibbosa, Valvulina oviedoiana, Ciclorbiculina compressa*) increased towards low-pH, high $C_{T,}$ and T_A values, presenting an increased abundance and lower sensitivity to OA. On contrary, sensitive species (e.g., *Thoculina* sp, *Sorites marginalis*, *Quinqueloculina subpoeyana*, *R. auberii*) are positioned at the right side of the plot (Fig. 3) close to high-pH, Ω Calcite and CO_3^{2-} values. The species *Rotorbinella rosea*, *Clavulina angularis*, *Quinqueloculina disparilis*, *Lachlanella carinata* and *Schlumbergerina alveoliniformis* present at the intermediated position in the graph decreased in abundance towards low-pH at a lower rate compared to the species on the right suggesting more tolerance. Axis 2 explained 19 % of the total variance, however no significant correlation to species distribution was found (p-value = 0.1).

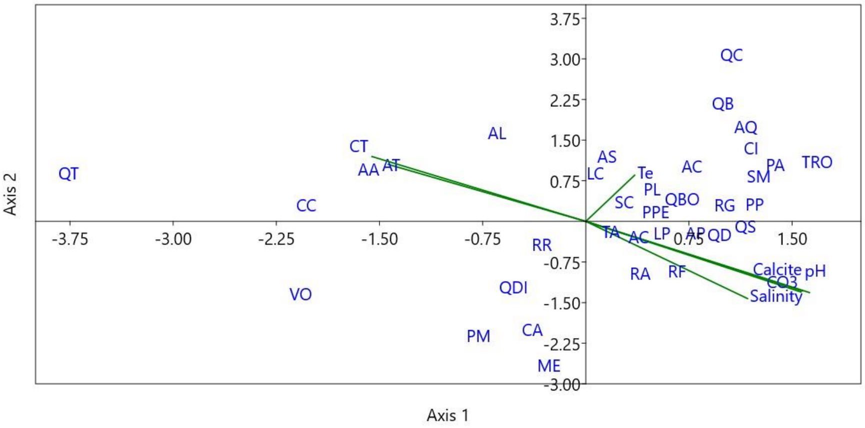

Figure 3 Canonical correspondence analysis diagram of the foraminiferal species (>3 %). Legend: AQ = *A. quadrilateralis*, AC = *A. carinata*, AL = *A. gibbosa*, AA = *Ar. angulatus*, AP = *A. pacifica*, AC = *A. compressa*, CI = *Cibicidoides* sp, CA = *C. angularis*, CC = *C. compressa*, LC = *L. carinata*, LP = *L. proteus*, ME = *M. elongata*, PPE = *P. pertustus*, PP = *P. planatus*, PA = *P. acervalis*, PM = *P. mediterranensis*, PL = *P. linneiana*, QBO = *Q. bosciana*, QC = *Q. carinatastriata*, QB = *Q. berthelotiana*, *QD* = *Q. distorqueata*, QDI = *Q. disparilis*, QS = *Q. subpoeyana*, QT = *Q. tricarinata*, RF = *R. floridana*, RG = *R. globularis*, RR = *R. rosea*, RA = *R. auberii*, AS = *S. alveoliniformis* , SM = *S.marginalis*, SC = *S. corrugata*, TA = *T. agglutinans*, TRO = *Trochulina* sp,VO = *V. oviedoiana*, Calcite = Ω Calcite, CO3 = CO_3^{2-}, Te = temperature.

The distribution of functional groups against changing pH is represented in Fig. 4. The symbiont-bearing taxa (Fig. 4a, R^2 = 0.54, p-value = 0.00) presented lower sensitivity to OA conditions increasing in relative abundance towards low-pH. The small miliolids (Fig. 5c, R^2 = 0.42, p-value = 0.00), opportunistic (Fig. 4d, R^2 = 0.28, p-value = 0.00), and small rotaliids taxa (Fig. 4a, R^2 = 0.36, p-value = 0.00) decreased in relative abundance towards low-pH conditions, presenting higher sensitivity. Kruskal-Wallis analysis reveal that the observed variation was statistically significant for most taxonomic metrics: Symbiont-bearing (chi-squared = 13, df = 3, p-value = 0.00), small miliolids (chi-squared = 12, df = 3, p-value = 0.00), opportunistic (chi-squared = 16, df = 3, p-value = 0.00), and small rotaliids (chi-squared = 9, df = 3, p-value = 0.00) and H (chi-squared = 19, df = 3, p-value = 0.00). Specifically, post hoc Dunn test revels that the significant changes occurred mainly between present day (~ 8.1 pH units) and extremely low-pH conditions (≤ 7.6 pH units) representing conditions beyond those predicted by the end of 21st century: Symbiont-bearing (z = −2.38, p-value = 0.01), small miliolids (z = 2.7, p-value = 0.00), and opportunistic (z= 2.4, p-value = 0.01). For small rotaliids taxa the significance was observed between low-intermediate acidification scenarios (~7.9 pH units), at which the group presented a higher contribution, and extremely low-pH conditions (≤ 7.6 pH units) where a strong decrease was observed with the other metrics (z = 1.7, p-value = 0.00). No significance was observed for agglutinated foraminifera (chi-squared = 2, df = 3, p-value = 0.5), which also did not present significant correlation with changing pH (Fig. 4e, $R^2 = 0.11$, p-value = 0.1). Raw data of functional and test type group are presented in table S2.

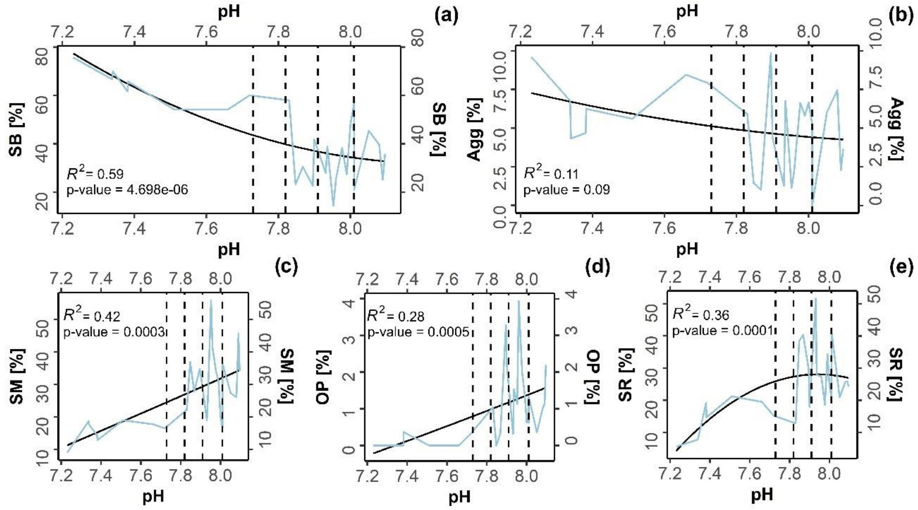

Figure 4 Variation of functional groups against changing pH. The black line represents the second-order polynomial model fits along with the R^2 value and the blue line represents the raw values obtained from in situ assemblages. Dashed lines demark predicted pH values at the end of this century following the Coupled Model Intercomparison Project Phase Six (CMIP6) predictions for Shared Socioeconomic Pathways (SSP1-2.6: 8.01 pH units; SSP2-4.5: 7.91 pH units; SSP3-7.0: 7.82 pH units, and SSP4: 7.73 pH units).

All taxonomic metrics presented a gradual decrease towards low-pH waters. On average, H′ ranged from 3.9 to 1.6 (Fig. 5a, $R^2 = 0.72$, p-value = 4.8^{-08}); S from 71 to 11 (Fig. 5b, $R^2 = 0.67$, p-value = 3.3^{-07}); J’ from 0.9 to 0.6 (Fig. 5c, $R^2 = 0.64$, p-value = 9.5^{-07}), and foraminifera density from 2167 to 36 ind./ml (Fig. 5d, $R^2 = 0.22$, p-value = 0.02). Kruskal-Wallis analysis revealed that the observed variation was statistically significant for all taxonomic metrics: N (chi-squared = 14.5, df = 3, p-value = 0.00), S (chi-squared = 20, df = 3, p-value = 0.00), J’ (chi-squared = 15, df = 3, p-value = 0.00) and H (chi-squared = 19, df = 3, p-value = 0.00). However as observed for functional and test type groups, the post hoc Dunn test revealed that significant changes occurred mainly between present day and extremely low-pH conditions: N (z = 2.2, p-value = 0.02), S (z = 3.4, p-value = 0.00), J (z = 3.1, p-value = 0.00), and H (z= 3.4, p-value = 0.00). No significant difference was observed for any taxonomic metric at low-intermediate acidification scenarios (SSP1-2.6 and SSP2-4.5), and only S differed significantly between present day and high acidification scenarios (Fig. 5b, SSP3-7.0 and SSP5-8.5, z = 2.1, p-value = 0.03). The taxonomic metrics were also plotted against changing Ω-Calcite for comparison with previous studies (e.g., Pettit et al., 2013, 2015, Martinez et al., 2018), however the obtained correlations were lower than those observed for pH (Fig. S1).

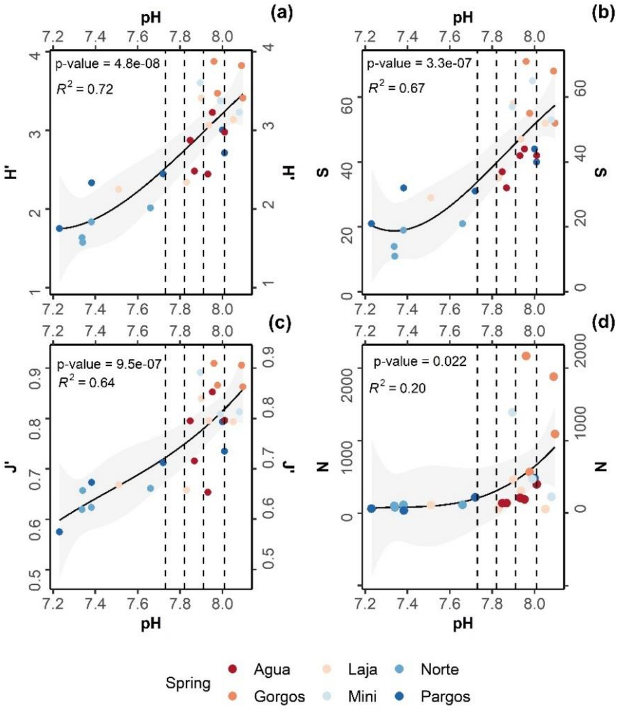

Figure 5 Relationships between pH and (a) Shannon-Weiner Diversity Index, (b) foraminiferal density, (c) Pielou's evenness, and (d) species richness. The black lines represent second-order polynomial model fits, and grey areas mark 95 % confidence intervals. Dashed lines demark predicted pH values at the end of this century following the Coupled Model Intercomparison Project Phase Six (CMIP6) predictions for Shared Socioeconomic Pathways (SSP1-2.6: 8.01 pH units; SSP2-4.5: 7.91 pH units; SSP3-7.0: 7.82 pH units, and SSP4: 7.73 pH units).

The hierarchical clustering based on foraminifera abundances revealed 7 assemblages, which corresponded well to functional and test type group distributions (Fig. 4), changes in carbonate water chemistry (Table 1) and taxonomic metrics (Fig. 5). A good representation of assemblage group's structure is present in nMDS plot (Fig. 6, 2D Stress: 0.06). Assemblages "f" and "e" consisted of samples retrieved at the higher pH conditions (8.1–7.9 pH units). Assemblages "g" and "d' comprised of samples retrieved at intermediated pH conditions (8.08-7.72 and 8-7.85, respectively). Assemblage "c" and assemblages "b" and "a" comprised samples retrieved living at extremely low-pH conditions of 8–7.51 and 7.66–7.23, respectively. The reduction of diversity, richness, and evenness along with decreasing pH can be observed from the left to the right part of the diagram (Fig. 6). An increase in symbiont-bearing and decrease in other groups also occurs towards the right part of the plot. SIMPER analysis reveals that the species *Ar. angulatus* whose relative contribution increased towards low-pH conditions was the major contributor to the forming groups, except assemblages "e" and "f" that were dominated by sensitive species that did not occur at low-pH (e.g., *Trochulina* sp, *Sorites marginalis*, *Quinqueloculina subpoeyana*, *R. auberii*). All species which are predominantly responsible for each group are listed in table S3.

In comparison to future projections, the highest dissimilarity (> 80 %) was observed between assemblages living close to present-day conditions (assemblage "e") and at the center of discharge, representing conditions beyond those projected for the end of the 21st century (assemblages "a" and "b"). Moderate similarity (47 %) was still observed for samples living at present-day (8.1 pH units), low-intermediate acidification (~ 7.9 pH units, SSP1-2.6 and SSP2-4.5), and high acidification scenarios (7.8-7.7 pH units, SSP3-7.0 and SSP5-8.5).

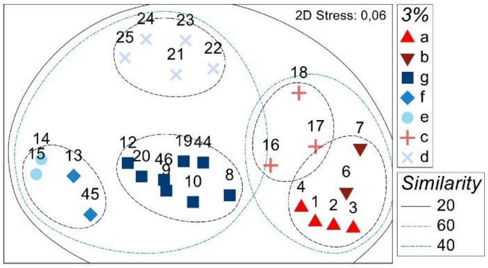

Figure 6 Non-metric multidimensional scaling (nMDS) ordination plot of 26 sampling stations of benthic foraminifera from Puerto Morelos.

Considering the consistency in the data analyses, we observed that under the most conservative projections (SSP1-2.6; SSP2-4.5) foraminifera assemblages did not display considerable changes in taxonomic metrics, presenting a moderate similarity (~50 %) to assemblages living at present-day conditions. For projections SSP3-7.0 and SSP5-8.5, moderate similarity was also observed, but the analyzed assemblages presented a significant decrease in richness S, indicating that foraminifera assemblages are likely to be affected under high acidification scenarios. To a species level, the symbiont-bearing taxa presented relatively higher resistance when compared to other functional groups, while agglutinated foraminifera were not measurably influenced by changes in pH.

3.3 Taphonomical and assemblage test size analysis

High-pH stations (~8.1 pH units) at PM are relatively pristine, however, this gradually changes as the effects of exudated waters increase. Linear correlations (Fig. 7b) show that dissolution ($R^2 = 0.55$, p-value = 0.00), and to a lesser extent, breakage ($R^2 = 0.30$, p-value = 0.00), increased with reducing pH until 7.8 units, where high levels of taphonomical alteration stated to occur. In respect to species distribution, the regression analysis shows a high correlation between the occurrence of some species and changing pH. Specifically, *Ar. angulatus* was responsible for 73 % of the dissolution observed in the samples ($R^2 = 0.73$, p-value = 0.00).

Along the gradient of changing carbonate chemistry, a significant change in foraminiferal assemblage test size was observed (Kruskal-Wallis, chi-squared = 16, df = 3, p-value = 0.00). A gradual decrease in the abundance of tests with smaller surface area and a relative increase of larger tests is observed towards low-pH sites (Fig. 7, R^2 = 0.73, p-value = 0.00). The post hoc Dunn's test reveals that only the differences between present-day and extremely low-pH conditions, which are beyond the predicted to the end of the 21st century were significant (z = -2.7, p-value = 0.00). Specifically, average test size in the assemblage more than tripled when compared to present-day conditions (from 0.33 ± 0.2 to 0.87 ± 0.14 mm^2). This abrupt change can be visualized in Fig. 6a, likely responding to changes in faunal composition rather than interspecific changes in species size. As observed in taphonomical analysis, linear correlation with respect to dominant taxa coverage, i.e., the species *Ar. angulatus*, shows a high and significant correlation of this species to changes in average assemblage test size (Fig. 7c, R^2 = 0.89, p-value = 0.00). Raw data of assemblage average test size, and taxonomic metrics are available in table S4.

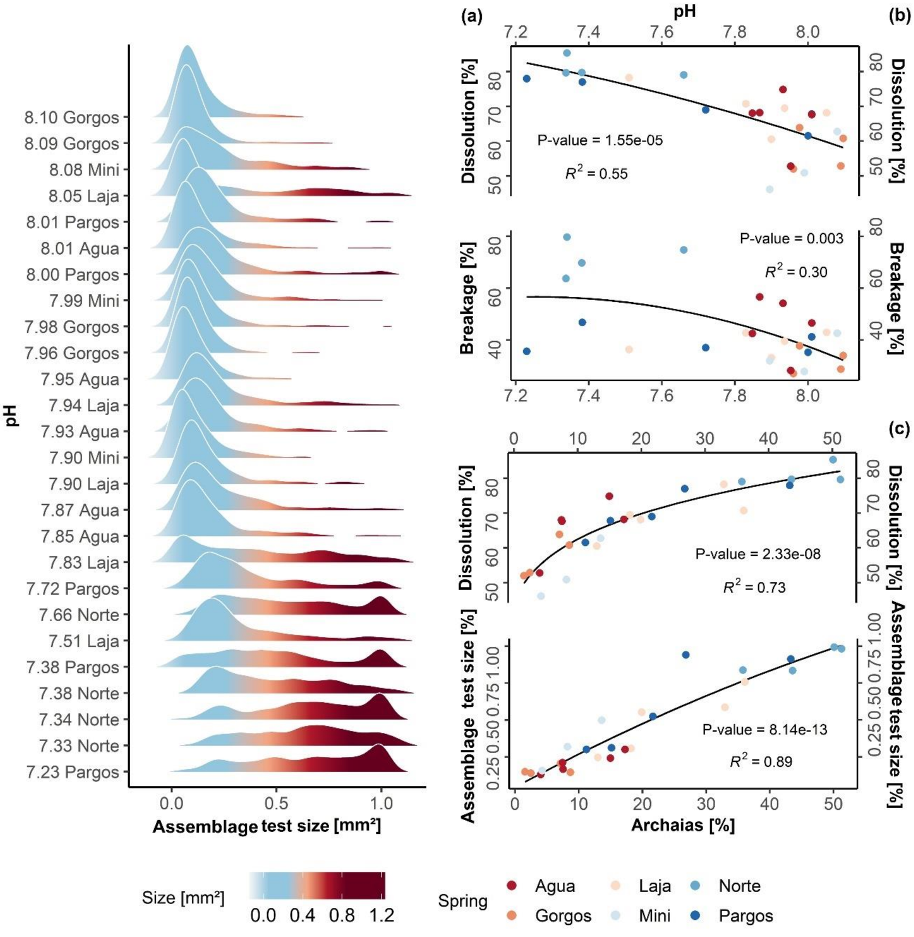

Figure 7 The (a) density plot of assemblage test size, (b) variation of dissolution and breakage against changing pH, and (c) variation of dissolution and average assemblage test size against *Archaias angulatus* relative contribution. The black lines represent second-order polynomial model fits along with the R^2 value and p-value (b; c). Dashed lines demark stations under high taphonomical alteration.

3.4 X-ray MicroCT

The X-ray MicroCT (Fig. 8a-d) analysis revealed that despite having a similar size (0.80 ± 0.05 mm^3), and volume (0.06 ± 0.02 mm^3) the specimens present at low-pH conditions (7.1 pH units) were on average 46 % less dense (2.4 ± 0.2 to 1.30 ± 0.03 g/cm^3) than the specimens present at high-pH conditions (Welch Two Sample t-test, t = 8.1204, df = 3.0808, p-value = 0.0035). Yet, no significant (Two Sample t-test, t = -1.4378, df = 6, p-value = 0.2) difference in chamber wall thickness was observed (0.050 ± 0.006 mm^3). The differences in internal density can be seen in Fig. 8a and 8b representing 2 specimens living in high and low-pH conditions, respectively. The external differences of these same individuals are represented in the 3D volume rendering at Fig. 8c and 8d. Raw data of test density, chamber wall thickness, test volume, and test diameter measured in *Ar. angulatus* individuals are listed in table S5.

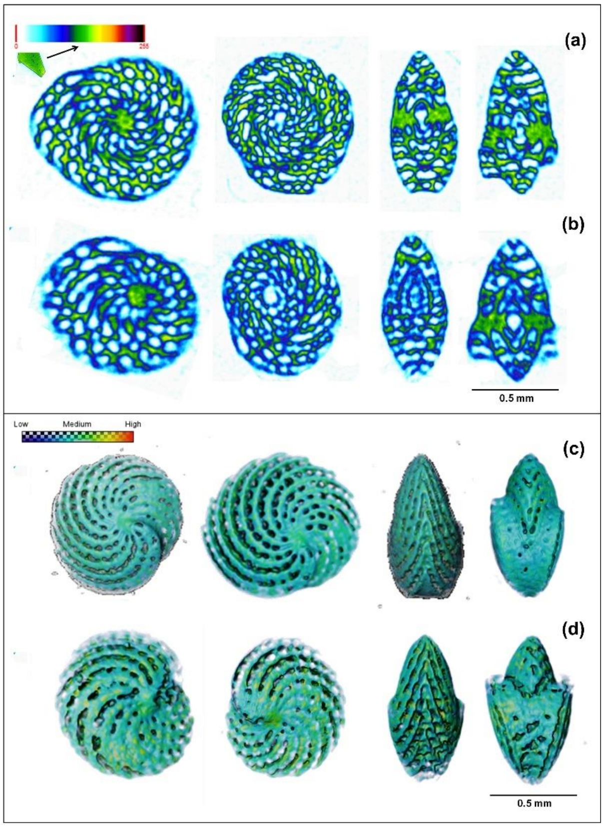

Figure 8 - Comparison between X-ray microCT images with color code as a function of calcite density. The specimen living at ~ 7.96 pH units (a) presents a higher calcite density when compared with low ~ pH 7.11 individual (b). The 3D Volume rendering in function of calcite density for the same individuals living at the high (c) and low-pH conditions (d). Note that individual at "d" living under low-pH presents a test with incomplete parts and blurred edges, which demonstrates a lower density.

4 Discussion

Under the two most conservative acidification projections (Fig. 5a-d) foraminifera assemblages in PM did not display considerable changes, while at high acidification scenarios a significant decrease in species richness was observed. These results indicate that benthic foraminifera are unlikely affected by pH decreases of ~ 0.2, but certainly respond adversely to higher acidification levels (~ 0.4 pH units). These findings are consistent with previous observations from other naturally high pCO_2 sites in which taxonomic metrics decreased significantly with declining pH (Bernhard et al. 2009; Dias et al. 2010; Pettit et al., 2015; Dong et al., 2019, 2020). It is noteworthy, however that changes in assemblage composition did not follow the same pattern observed in these previous studies. Whereas the proportion of calcareous species usually decline with decreasing pH, they remained dominant (~90 %) under all projections in PM, suggesting a relatively higher resistance for these shallow-reef benthic assemblages.

The in-situ occurrence of calcifying foraminifera at high acidification scenarios (SSP3-7.0 and SSP5-8.5) have only been reported in the deep-sea near extensive CO_2 vents in the Wagner Basin (Pettit et al., 2013). At this site, a rich food supply and stable temperatures were considered to offset the effects of OA and a shift towards opportunistic assemblages was reported. The springs from PM also have high nutrient concentrations compared to the open waters in the region (Null et al., 2014; Crook et al., 2016), however, near spring assemblages did not change towards opportunistic dominated assemblages, suggesting that the nutrient availability does not exert a major control at this site. Rather, the high-pH assemblages heavily dominated by small calcareous forms were replaced by larger symbiont-bearing species near the springs (Fig. 4a-e). Symbiont-bearing species are known to be sensitive to high nutrient loading, likely because of changes in turbidity/light regimes and their dependence on algal symbionts to enhance growth and calcification (Hallock et al., 2003). At PM despite higher nutrient levels the waters at the springs are clear and light regimes are not reduced.

The chemical conditions at PM, along with the physiology of calcification in foraminifera may also explain the lack of sensitivity to the mid-range pH conditions. Recent calcification models demonstrate that foraminifera are able to manipulate pH to control the speciation of inorganic carbon parameters during calcification (De Nooijer et al., 2009; Toyofuku et al., 2017; De Goyese et al., 2021; Geerken et al., 2022). Specifically, the proton-pumping based model (Toyofuku et al., 2017) shows that at the external environment, a decrease in pH (~ 6.9 pH units) induces the transformation of CO_3^{2-} and bicarbonate (HCO^{3-}) into CO_2, whereas at the site of calcification the elevated pH (~ 9 pH units) results in the opposite shift into CO_3^{2-}. As foraminifera induce pH changes exceeding the predicted to SSP1-2.6 and SSP2-4.5, low-intermediate acidification scenarios are in fact unlikely to impair foraminiferal calcification. As such, these

https://doi.org/10.5194/bg-2022-91
Preprint. Discussion started: 13 April 2022

models also suggest that increased CO_2 might favor foraminifera by increasing C_T, which is notably higher towards the springs in PM (Table 1).

It is also suggested that higher C_T might favor symbiont-bearing foraminifera at low-pH (~ 7.8) by inducing CO_2 fertilization effects and increased activity of symbionts (Fujita et al., 2011), which is in agreement with our results. For example, from assemblage "e" and "f" (~ 8.1 pH units) to "g" and "d" (~7.7 pH, SIMPER analysis) symbiont-bearing species including (1) *Ar. angulatus* (chlorophyte-bearing), increased in abundance from 4–7 % to 10–13 %, (B) *Amphistegina gibbosa* (diatom-bearing), increased in some stations from 4 % to 7 %, and (C) *Cyclorbiculina compressa* (chlorophyte-bearing) that presented low contribution < 3 % at high-pH stations also increased in relative contribution to 4 % at intermediated pH. Additionally, the high C_T and T_A might also raise local pH and carbonate saturation during photosynthesis, even if only on the scale of an individual organism at the foraminiferal shell surface, which could also increase the symbiont-bearing resistance. Under ambient conditions, Köhler-Rink and Kühl. (2000) observed that photosynthesis increased the pH at the shell surface up to 8.6. These species were placed close to the C_T and T_A vectors at the CCA diagram, which highlights their association to higher dissolved carbon and alkalinity content (Fig. 3). In accord, laboratory-controlled experiments have also shown that the symbiont-bearing *Ar. angulatus* (Stuhr et al., 2021) and *Amphistegina* sp (Prazeres et al., 2015) can calcify and live under relatively low-pH conditions (~ 7.6 pH units).

The ability of foraminifera to function and calcify near the springs may also be related to the site-specific natural pH variability to which the species are exposed. For example for many coastal/transitional areas characterized by high pCO_2 variability foraminifera seem to be more resilient and acclimated to changing conditions including low-pH (Haynert et al., 2012; Charrieau et al., 2018). By discharging low-pH waters for millennia (Back et al., 1979) the foraminifera living near the spring have experienced a pH variability over a much longer timespan than the life span of individual organisms (Martinez et al., 2018). Specifically, as reef-dwelling organisms, the foraminifera in PM experience a wide range of pH on daily and seasonal scales which might, at least to a certain extent, physiologically increase the species resilience to low-pH waters (Price et al., 2012). Moreover, in-situ recruitment and succession experiments in PM showed that foraminifera were able to calcify and increased in density over the investigated period (14 months) (data from Laja and Gorgos springs , Crook et al., 2016). As observed by Martinez et al. (2018) calcareous species at PM persist even at extreme acidification levels (~ 7.1 pH units).

In our work we observed that *Ar. angulatus* doubled its relative contribution at low-pH (~ 8–7.8) (e.g., 13 % in assemblage "g", table S3) and almost tripled at extremely low-pH (>7.7) (e.g., 30 % in assemblage 'a", table S3) compared to assemblages living at 8.1 pH units (e.g., 4 % in assemblage "e", table S3). Due to its strong increase towards the springs, we employed an X-ray microCT analysis (Fig. 8a-d) to investigate possible acclimation patterns that could explain the observation.

The analysis revealed that despite having similar size (0.80 ± 0.05 mm^3), volume (0.06 ± 0.02 mm^3), and chamber wall thickness (0.050 ± 0.006 mm^3) the specimens found at low-pH conditions (7.1 pH units) were on average 46 % less dense (2.40 ± 0.2 to 1.30 ± 0.03 g/cm^3) than the specimens present at high-pH conditions (7.96 pH units). This demonstrates that the species is able to calcify in low-pH conditions beyond the predicted for the late 21st century albite at lower density. The lower density however indicates that

Archaias individuals were not capable to acclimate sufficiently to maintain ambient present day calcification efficiency. These results are in agreement with Knorr et al. (2015) that observed a 50 % decrease in *Ar. angulatus* size at 7.6 pH units, and a consequent decrease of 85 % in the production of high-Mg calcite by this species. Further analyses are needed for a better understanding of *Archaias* biological thresholds, but this ability to calcify at even 7.1 pH units certainly provides a competitive advantage over other species that are less robust calcifiers.

Considering that foraminifera are a crucial component of reef sediment production (Langer et al., 1997; Langer, 2008), including *Ar. angulatus* in the Caribbean region, our results support previous findings that reef-building carbonate production and accumulation are likely to decrease under future scenarios, even in the tropics (*Knorr* et al., 2015; Eyre et al., 2018; Kuroyanagi et al., 2021). Specifically, we also observed a decrease in foraminifera density (Fig.5d) and therefore in carbonate accumulation as foraminifera tests in the sediments. As OA intensifies, symbiont-bearing taxa, which demonstrated higher resistance to low-pH, will likely still represent major contributors in the Caribbean and Gulf of Mexico sediments where species like *Ar. angulatus* dominate (Culver and Buzas, 1982). In contrary, the high sensitivity of *Rosalina* spp, *Quinqueloculina* spp, *Triloculina* spp, *Articulina* spp, and *Miliolinella* spp to low-pH highlighted their lower fitness in response to OA, demonstrating that changes in abundance of small taxa can be used as bioindicators to monitor the effects of OA.

Since *Ar. angulatus* showed lower density close to the low-pH springs and hence is negatively impacted by the low-pH, the species relative increase in contribution towards the springs is probably associated with the high preservation potential of its tests. Their tests are larger, thicker, and reinforced by internal partitions (pillars), therefore more likely to be preserved in the sediment (Martin, 1986; Cottey and Hallock, 1988). This is confirmed by the performed regression analysis as the species relative contribution explains 88 % of assemblage test size and 73 % of dissolution occurrence in the samples (Fig. 7c). In fact, changes were so abrupt that shifts in the assemblage test size and functional groups were clearly observed at ≤ 7.83 pH units (Fig. 7a), when the symbiont-bearing taxa contribution also started to increase (Fig. 4a). At this point preservation thresholds of smaller taxa seemed to be crossed, and their relative decrease near the springs is likely related to higher rates of breakage and dissolution (Present study, Martinez et al., 2018).

The relative contribution of agglutinated foraminifera slightly increased towards low-pH (Fig. 4b), but they did not compensate for the decline in calcareous species (Fig. 4a–e). Since the particles available for the agglutinated tests are made of carbonate and under low-Ω waters are also prone to dissolve that may affect the agglutinated species. Interestingly, agglutinated foraminifera also presented species-specific responses to acidification similar to the calcareous foraminifera. For example, *Valvulina oviedoiana* increased towards low-pH while *Textularia agglutinans* presented a strong decrease. Since acidification is expected to have little direct effect on agglutinated foraminifera the observed interspecific behavior is also probably associated with preservation potential. The variation of agglutinating material (e.g., mucopolysaccharide), structure (e.g., fibrous, strands, foam-like masses), and size of granular particles (e.g., fine, and coarser) are essential to determine the preservation and accumulation of agglutinated tests (Bender and Hemleben, 1988). The most important agglutinated species, in our study e.g., *T. agglutinans*, *C. angulata*, and *V. oviedoiana* use calcitic cement as the agglutinating material of particles, which probably assigns a higher resistance to dissolution (Bender, 1995). Among these, *T. agglutinans* lower resistance likely responds to its smaller size, which implies higher dissolution (Bender, 1995). Altogether, we observe that until ~ 7.8 pH units foraminifera physiology was a main driver of foraminifera distribution, whereas at ≤ 7.7 pH units (Fig. 7b) the preservation potential became an important factor affecting the distribution of both calcareous and agglutinated tests.

Although *postmortem* degradation likely occurs at higher rates near the springs the distribution of species still provide a good representation of the fauna over a short ecological time. That is also the case for most symbiont-bearing taxa, as the relative contribution of individual species discussed above increase towards low-pH. However, we cannot exclude the possibility that a higher accumulation of *Ar. angulatus* tests could be responsible for an overestimation in symbiont-bearing taxa density. In this case, species richness would be more reliable to the interpretation of assemblage responses, which was the only parameter to decrease significantly at < 7.7 pH units (Fig. 5b), validating that in general foraminifera are less likely to acclimate under high acidification scenarios. These results bring serious implications as SSP3-7.0 and SSP5-8.5 scenarios also predict substantial increases of sea surface temperature (Kwiatkowski et al., 2020), which combined to surface OA might critically decrease the tolerance of foraminifera (reviewed in Kawahata et al., 2019). Recently, Bernhard et al. (2021) observed that foraminiferal assemblages presented the lowest number of species and abundances under a triple-stressed (low-pH/O_2 and high temperature) treatment demonstrating the synergetic effects of these variables. As observed in PM, agglutinated foraminifera were relatively more resistant than calcareous taxa.

For emissions beyond the predicted to the end of 21st century all taxonomic metrics decreased significantly, and calcareous species with higher preservation potential like *C. compressa* and *Ar. angulatus* comprised up 50–60 % of assemblage composition. These calcareous taxa were still found probably due to high T_A levels, which was also considered to likely limit the dissolution rates of *Ar. angulatus* and other porcelaneous tests in the springs coast of Florida, where numerous spring-fed rivers emerge from Eocene and Oligocene limestone and dolostone substrata (Amergian et al., 2022). If we restricted the analysis to only pristine, well-preserved tests, the taxonomic metrics at 7.6-7.2 (Fig. 6) would be much lower and more similar to those presented by Uthicke, Momigliano, and Fabricius (2013), in which foraminifera were almost absent at sites with ≤ 7.9 pH units.

5 Conclusion

This work shows that despite their life-long exposure to low-pH conditions, tropical foraminifera species will be negatively affected under the high acidification scenarios (SSP3-7.0 and SSP5-8.5) for the end of the 21st century. Species-specific responses in foraminiferal assemblages were observed and as the oceans become more acidic, reef foraminiferal assemblages might gradually shift towards larger, symbiont-bearing species and agglutinating foraminifera. The species *Ar. angulatus*, which is known to be dominant in warm, oligotrophic areas of the Caribbean and Gulf of Mexico are able to calcify at pH conditions lower than those projected by SSP5-8.5, however, the observed lower density of the pristine tests suggests that reef carbonate budget might decrease as this species represent a major carbonate producer at these areas. Considering the observed trends of increasing average assemblage test size and the results of multivariate faunal analysis (SIMPER, CCA), our results demonstrate the key role smaller foraminifera have as bioindicators to monitor the effects of OA, as their high sensitivity to dissolution makes them first responders to ongoing OA.

6 Data availability

All data related to this study are given in the Supplement data files that accompany this paper.

7 Author contribution

DF, AP and CFB conceived of and designed the study. DF performed the faunal and statistical analysis. OMA and RTL conducted the Micro-CT experiments. DF, AP and CFB analyzed the data. DF, AP, CFB prepared the original draft of the manuscript with writing, and OMA and RTL reviewed and edited.

8 Competing interest

We declare that this manuscript has no conflict of interest.

9 Acknowledgments

This study was funded by the National Science Foundation-1040952 (to AP). DF thanks the scholarship of the National Council for Scientific and Technological Development (CNPq) No. 132210/2020-7. The funders had no role in the study design, data collection and analysis, decision to publish, or preparation of the paper. DF thanks Pamela Hallock and Heitor Evangelista for their helpful comments and suggestions.

10 References

Abu-Zied, R. H., Al-Dubai, T. A., and Bantan, R. A.: Environmental conditions of shallow waters alongside the southern Corniche of Jeddah based on benthic foraminifera, physico-chemical parameters and heavy metals, J. Foramin. Res., 46(2), 149–170, https://doi.org/10.2113/gsjfr.46.2.149, 2016.

Amergian, K. E., Beckwith, S., Gfatter, C., Selden, C., Hallock, P.: Can areas of high alkalinity freshwater discharge provide potential refugia for marine calcifying organisms?, J. Foramin. Res., 52(1), 63–76, https://doi.org/10.2113/gsjfr.52.1.60, 2022.

Andersson, A.J., Kline, D.I., Edmunds, P.J., Archer, S.D., Bednarsek, N., Carpenter, R.C., Chadseym, M., Goldstein, P., Grottoli, A.G., Hurst, T.P., King, A.L., kubler, J.E., Kuffner, I.B., Mackey, K. R. M., MENGE, B.A., Paytan, A., Riebesell, U., and Zimmerman, A.S.R.: Understanding ocean acidification impacts on organismal to ecological scales, Oceanography, 28(2), 16–27, https://doi.org/10.5670/oceanog.2015.27, 2015.

Back, W., and Hanshaw, B. B.: Comparison of chemical hydrogeology of the carbonate peninsulas of Florida and Yucatan, J. Hydrol., 10, 330–368, https://doi.org/10.1016/0022-1694(70)90222-2, 1970.

Back, W., Hanshaw, B. B., Pyle, T. E., Plummer, L. N., and Weidie, A. E.: Geochemical significance of groundwater discharge and carbonate solution to the formation of Caleta Xel Ha, Quintana Roo, Mexico, Water Resour. Res., 19(6), 1521–1535, https://doi.org/10.1029/WR015I006P01521, 1979.

Barbosa, C. F., Prazeres, M., Padovani, B., and Seoane, J. C. S.: Foraminiferal assemblage and reef check census in coral reef health monitoring of East Brazilian margin, Mar. Micropaleontol., 73, 62–69, https://doi.org/10.1016/j.marmicro.2009.07.002, 2009.

Barbosa, C. F., Ferreira, B. P., Seoane, J. C. S., Oliveira-Silva, P., Gaspar, A. L. B., Cordeiro, R. C., and Soares-Gomes, A.: Foraminifer-based coral reef health assessment for southwestern Atlantic offshore archipelagos, Brazil, J. Foramin. Res., 42(2), 169–183, https://doi.org/10.2113/gsjfr.42.2.169, 2012.

https://doi.org/10.5194/bg-2022-91
Preprint. Discussion started: 13 April 2022

Beddows, P. A., Smart, P. L., Whitaker, F. F., and Smith, S. L.: Decoupled fresh – saline groundwater circulation of a coastal carbonate aquifer: Spatial patterns of temperature and specific electrical conductivity, J. Hydrol., 346, 18–32, https://doi.org/10.1016/j.jhydrol.2007.08.013, 2007.

Bender, H., and Hemleben, C.: Constructional aspects in test formation of some agglutinated foraminifera. Abh. Geol. B.-A., 13–22, 1988.

Bender, H.: Test structure and classification in agglutinated Foraminifera. In: Kaminski, M. A., Geroch, S. and Gasiñski, M. A., Eds., Proceedings of the Fourth International Workshop on Agglutinated Foraminifera, Kraków Poland, September 12–19, 1993, 27–70. Grzybowski Foundation Special Publication, 3, 1995.

Bernhard, J. M., Barry, J. P., Buck, K. R., and Starczak, V. R.: Impact of intentionally injected carbon dioxide hydrate on deep-sea benthic foraminiferal survival, Global Change Biol., 15(8), 2078–2088, https://doi.org/10.1111/j.1365-2486.2008.01822.x, 2009.

Bernhard, J. M., Wit, J. C., Starczak, V. R., Beaudoin, D.J., Phalen, W.G., and Mccorkle, D.C.: Impacts of multiple stressors on a benthic foraminiferal community: a long-term experiment assessing response to ocean acidification, hypoxia and warming, Front. Mar. Sci., 8, 1–18. https://doi.org/10.3389/fmars.2021.643339, 2021.

Charrieau, L. M., Filipsson, H. L., Nagai, Y., Kawada, S., Ljung, K., Kritzberg, E., and Toyofuku, T. Decalcification and survival of benthic foraminifera under the combined impacts of varying pH and salinity, Mar. Environ. Res., 138, 36–45, https://doi.org/10.1016/j.marenvres.2018.03.015, 2018.

Clarke, K. R. and Gorley, R.N.: PRIMER v6: User manual/tutorial, PRIMER-E Ltd., Plymouth, UK, 2006.

Cottey, T. L. and Hallock, P.: Test surface degradation in *Archaias angulatus*, J. Foramin. Res., 8(3), 187–202, Https://doi.org/ 10.2113/gsjfr.18.3.187, 1988.

Crook, E. D., Potts, D., Hernandez, L., and Paytan, A.: Calcifying coral abundance near low-pH springs: implications for future ocean acidification, Coral reefs, 31, 239–245, https://doi.org/10.1007/s00338-011-0839-y, 2012.

Crook, E. D., Cohen, A. L., Rebolledo-Vieyra, M., Hernandez, L., and Paytan, A.: Reduced calcification and lack of acclimatization by coral colonies growing in areas of persistent natural acidification, PNAS, 110, 27, 11044–11049, https://doi.org/10.1073/pnas.1301589110, 2013.

Crook, E. D., Kroeker, K. J., Potts, D. C., and Rebolledo-Vieyra, M.: Recruitment and succession in a tropical benthic community in response to in-situ ocean acidification, PLoS ONE, 11, e0146707, https://doi.org/10.1371/journal.pone.0146707, 2016.

Culver, S. J., and Buzas, M. A.: Distribution of Recent benthic foraminifera in the Caribbean area. Smithsonian Institution Press, Washington, https://doi.org/10.5479/si.01960768.14.1, 1982.

Cushman, J.A.: The foraminifera of the Atlantic Ocean. Bulletin 104, Smithsonian Institution. USNM. v. 2, Netherlands, Reprint 1970, 1929.

De Goeyse, S., Webb, A. E., Reichart, G. J., and De Nooijer, L. J.: Carbonic anhydrase is involved in calcification by the benthic foraminifer *Amphistegina lessonii*, Biogeosciences, 18, 393–401. https://doi.org/10.5194/bg-18-393-2021, 2021.

De Nooijer, L. J., Langer, G., Nehrke, G., and Bijma, J. (2009). Physiological controls on seawater uptake and calcification in the benthic foraminifer *Ammonia tepida*, Biogeosciences, 6, 2669–2675, https://doi.org/10.5194/bg-6-2669-2009, 2009.

Dias, B. B., Hart, M. B., Smart, C. W., and Hall-Spencer, J. M.: Modern seawater acidification: the response of foraminifera to high-CO_2 conditions in the Mediterranean Sea, J. Geol. Soc. London, 167, 843–846, https://doi.org/10.1144/0016-76492010-050, 2010.

Dickson, A. G., Sabine, C. L., and Christian, J. R.: Guide to best practices for ocean CO_2 measurements, North Pacific Marine Science Organization, Sidney, BC, Canada, 2007.

Doney, S.C., Busch, D.S., Cooley, S. R., and Kroeker, K. J.: The impacts of ocean acidification on marine ecosystems and reliant human communities, Annu. Rev. Environ. Resour., 45, 83–112, 2020, https://doi.org/10.1146/annurev-environ-012320-083019, 2020.

Dong, S., Lei, Y., Li, T., and Jian, Z.: Changing structure of benthic foraminiferal communities due to declining pH: Results from laboratory culture experiments, Sci. China Earth Sci., 62, 1151–1166, https://doi.org/10.1007/s11430-018-9321-6, 2019.

Dong, S., Lei, Y., Li, T., and Jian, Z.: Response of benthic foraminifera to pH changes: Community structure and morphological transformation studies from a microcosm experiment, Mar. Micropaleontol., 156, 101819, https://doi.org/10.1016/j.marmicro.2019.101819, 2020.

https://doi.org/10.5194/bg-2022-91
Preprint. Discussion started: 13 April 2022

Doo, S. S., Hamylton, S., Finfer, J., and Byrne, M.: Spatial and temporal variation in reef-scale carbonate storage of large benthic foraminifera: a case study on One Tree Reef, Coral reefs, 36, 293–303, https://doi.org/10.1007/s00338-016-1506-0, 2016.

Engel, B. E., Hallock, P., Price, R. E., and Pichler, T.: Shell dissolution in larger benthic foraminifers exposed to pH and temperature extremes: Results from an in-situ experiment, J. Foramin. Res., 45(2), 190–203, https://doi.org/10.2113/gsjfr.45.2.190, 2015.

Eyre, B.D., Cyronak, T., Drupp, P., De Carlos, E. H., Sach, J.P., and Andersson, A.J.: Coral reefs will transition to net dissolving before end of century, Science, 359, 6378, 908–911, https://doi.org/10.1126/science.aao1118, 2018.

Fujita, K., Hikami, M., Suzuki, A., Kuroyanagi, A., Sakai, K., Kawahata, H., and Nojiri, Y.: Effects of ocean acidification on calcification of symbiont-bearing reef foraminifers, Biogeosciences, 8, 2089–2098, https://doi.org/10.5194/bg-8-2089-2011, 2011.

Geerken, E., De Nooijer, L. J., Toyofuku, T., Roepert, A., Middelburg, J. J., Kienhuis, M. V. M., Nagai, Y., Polerecky, L., and Reichart, G. J.: High precipitation rates characterize biomineralization in the benthic foraminifer *Ammonia beccarii*, Geochim. Cosmochim. Acta, 318, 70–82, https://doi.org/10.1016/j.gca.2021.11.026, 2022.

Gischler, E., and Möder, A.: Modern benthic foraminifera on Banco Chinchorro, Quintana Roo, Mexico, Facies, 55, 27–35, https://doi.org/10.1007/s10347-008-0162-4, 2009.

Hallock, P., Lidz, B. H., Burkhard-Cockey, E. M., and Donnelly, K. B.: Foraminifera as bioindicators in coral reef assessment and monitoring: The FORAM Index, Environ. Monit. Assess., 81, 221–238, https://doi.org/10.1023/A:1021337310386, 2003.

Haynert, K., Schönfeld, J., Polovodova-Asteman, I., and Thomsen, J.: The benthic foraminiferal community in a naturally CO_2-rich coastal habitat in the southwestern Baltic Sea, Biogeosciences, 9, 4421–4440, https://doi.org/10.5194/bgd-9-7783-2012, 2012.

Hughes, T. P., Barnes, M. L., Bellwood, D. R., Cinner, J. E., Cumming, G. S., Jackson, J. B.C., Kleypas, J., Van De Leemput, I. A., Lough, J. M., Morrison, T. H., Palumbi, S. R., Van Nes, E. H., and Scheffer, M.: Coral reefs in the Anthropocene, Nature, 546, 82–90, https://doi.org/10.1038/nature22901, 2017.

IPCC, 2021: Climate Change 2021: The Physical Science Basis. contribution of working group I to the sixth assessment report of the intergovernmental panel on climate change [Masson-Delmotte, V., P. Zhai, A. Pirani, S.L. Connors, C. Péan, S. Berger, N. Caud, Y. Chen, L. Goldfarb, M.I. Gomis, M. Huang, K. Leitzell, E. Lonnoy, J.B.R. Matthews, T.K. Maycock, T. Waterfield, O. Yelekçi, R. Yu, and B. Zhou (eds.)]. Cambridge University Press. In Press.

Jones, R.W.: The challenger foraminifera – The Natural History Museum. Oxford University Press, London, 1994.

Kawahata, H., Fujita, K., Iguchi, A., Inoue, M., Iwasaki, S., Kuroyanagi, A., Maeda, A., Manaka, T., Moriya, K., Takagi, H., Toyofuku, T., Yoshimura, T., and Suzuki, A.: Perspective on the response of marine calcifiers to global warming and ocean acidification — Behavior of corals and foraminifera in a high CO_2 world "hot house", Prog. Earth Planet. Sci., 6(5), 1–37, https://doi.org/10.1186/s40645-018-0239-9, 2019.

Knorr, P. O., Robbins, L. L., Harries, P. J., Hallock, P., and Wynn, J.: Response of the miliolid *Archaias angulatus* to simulated ocean acidification, J. Foramin. Res., 45(2), 109–127, https://doi.org/10.2113/gsjfr.45.2.109, 2015.

Köhler-Rink, S., Kühl, M.: Microsensor studies of photosynthesis and respiration in larger symbiotic foraminifera. I The physico-chemical microenvironment of *Marginopora vertebralis*, *Amphistegina lobifera* and *Amphisorus hemprichii*, Mar. Biol., 137, 473–486, https://doi.org/ 10.1007/s002270000335, 2000.

Kroeker, K. J., Kordas, R. L., Crim, R., Hendriks, I. E., Ramajo, L., Singh, G. S., Duarte, C. M. and Gattuso, J.P.: Impacts of ocean acidification on marine organisms: quantifying sensitivities and interaction with warming, Global Change Biol., 19, 1884–1896, https://doi.org/10.1111/gcb.12179, 2013.

Kuroyanagi, A., Iriem T., Kinoshita, S., Kawahata, H., Suzuki, A., Nishi, H., Sasaki, O., Takashima, R., and Fujita, K.: Decrease in volume and density of foraminiferal shells with progressing ocean acidification, Sci. Rep., 11, 19988. https://doi.org/10.1038/s41598-021-99427-1, 2021.

Kwiatkowski, L., Torres, O., Bopp, L., Aumont, O., Chamberlain, M., Christian, J., Dunne, J., Gehlen, M., Ilyina, T., John, J., Lenton, A., Li, H., Lovenduski, N., Orr, J., Palmieri, J., Santana-Falcón, Y., Schwinger, J., Séférian, R., Stock, C., Tagliabue, A., Takano, Y., Tjiputra, J., Toyama, K., Tsujino, H., Watanabe, M., Yamamoto, A., Yool, A., and Ziehn, T. Twenty-first century ocean warming, acidification, deoxygenation, and upper ocean nutrient decline from CMIP6 model projections, Biogeosciences, 17, 3439–3470, https://doi.org/10.5194/bg-2020-16, 2020.

Langer, M. R., Lipps, J. H., Silk, M. T., and Lipps, J. H. Global ocean carbonate and carbon dioxide production: the role of reef foraminifera, J. Foramin. Res., 27(4), 271–277, https://doi.org/10.2113/gsjfr.27.4.271, 1997.

Langer, M. R.: Assessing the contribution of foraminiferan protists to global ocean carbonate production, J. Eukaryotic Microbiol., 55(3), 163–169, https://doi.org/10.1111/j.1550-7408.2008.00321.x, 2008.

Lida, Y., Takatani, Y., Kojima, A., and Ishii, M.: Global trends of ocean CO_2 sink and ocean acidification: an observation-based reconstruction of surface ocean inorganic carbon variables, J. Oceanogr., 77, 323–358, https://doi.org/10.1007/s10872-020-00571-5, 2021.

Lueker, T. J., Dickson, A. G., and Keeling, C. D.: Ocean pCO_2 calculated from dissolved inorganic carbon, alkalinity, and equations for K1 and K2: validation based on laboratory measurements of CO_2 in gas and seawater at equilibrium, Mar. Chem., 70, 105–119, https://doi.org/10.1016/S0304-4203(00)00022-0 , 2000.

Lüthi, D., Le Floch, M., Bereiter, B., Blunier, T., Barnola, J. M., Siegenthaler, U., Raynaud, D., Jouzel, J., Fischer, H., Kawamura, K., and Stocker, T. F.: High-resolution carbon dioxide concentration record 650,000-800,000 years before present, Nature, 453, 379–382, https://doi.org/10.1038/nature06949, 2008.

Martin, R. E.: Habitat and distribution of the foraminifer *Archaias angulatus* (Fichtel and Moll) (Miliolina, Soritidae), northern Florida Keys, J. Foramin. Res., 16, 3, 201–206, https://doi.org/10.2113/gsjfr.16.3.201, 1986.

Martinez, A., Hernández-Terrones, L., Rebolledo-Vieyra, M., and Paytan, A.: Impact of carbonate saturation on large Caribbean benthic foraminifera assemblages, Biogeosciences, 15, 6819–6832, https://doi.org/10.5194/bg-15-6819-2018, 2018.

Martinez, A., Crook, E. D., Barshis, D. J., Potts, D. C., Rebolledo-Vieyra, M., Hernandez, L., and Paytan, A.: Species-specific calcification response of Caribbean corals after 2-year transplantation to a low aragonite saturation submarine spring, Proceedings B, 286, 20190572, https://doi.org/10.6084/m9, 2019.

Milker, Y., and Schmiedl, G.: A taxonomic guide to modern benthic shelf foraminifera of the western Mediterranean Sea, Palaeontol. Electronica, 15(2), 1–134, https://doi.org/10.26879/271, 2012.

Moodley, L., Boschker, H. T. S., Middelburg, J. J., Pel, R., Herman, P. M. J., De Deckere, E., and Heip, C. H. R.: Ecological significance of benthic foraminifera: 13C Labelling experiments, Mar. Ecol. Prog. Ser., 202, 289–295, https://doi.org/10.3354/meps202289, 2000.

Murray, J.W.:Ecology and applications of benthic foraminifera. Cambridge University Press, Cambridge, New York., 2006.

Narayan, G. R., Reymond, C. E., Stuhr, M., Doo, S., Schmidt, C., Mann, T., and Westphal, H.: Response of large benthic foraminifera to climate and local changes: Implications for future carbonate production, Sedimentology, 69, 121–161, https://doi.org/10.1111/sed.12858, 2021.

Nehrke, G., Keul, N., Langer, G., De Nooijer, L. J., Bijma, J., and Meibom, A.: A new model for biomineralization and trace-element signatures of Foraminifera tests, Biogeosciences, 10, 6759–6767, https://doi.org/10.5194/bg-10-6759-2013, 2013.

Null, K. A., Knee, K. L., Crook, E. D., Sieyes, N. R., Rebolledo-Vieyra, M., Hernández-Terrones, L., and Paytan, A. Composition and fluxes of submarine groundwater along the Caribbean coast of the Yucatan Peninsula, Cont. Shelf Res., 77, 38–50, https://doi.org/10.1016/j.csr.2014.01.011, 2014.

Penã, V., Harvey, B. P., Agostini, S., Porzio, L., Milazzo, M., Horta, P., Gall, L.L., and Hall-Spencer, J.M. Major loss of coralline algal diversity in response to ocean acidification, Global Change Biol., 27(19), 4785–4798, https://doi.org/10.1111/gcb.15757, 2021.

Perry, E., Velazquez-Oliman, G., and Marin, L. The hydrogeochemistry of the karst aquifer system of the northern Yucatan peninsula, Mexico, Int. Geol. Rev., 44, 191–221, https://doi.org/10.2747/0020-6814.44.3.191, 2022.

Peters, G. P., Andrew, R. M., Canadell, J. G., Friedlingstein, P., Jackson, R. B., Korsbakken, J. I., Le Quéré, C., and Peregon, A.: Carbon dioxide emissions continue to grow amidst slowly emerging climate policies, Nat. Clim. Change, 10, 3–6, https://doi.org/10.1038/s41558-019-0659-6, 2020.

Petit, J. R., J. Jouzel, Raynaud, D., Barnola, J. M., Basile, I., Bender, M., Chappellaz, J., Davis, M., Delaygue, G., Delmotte, M., Kotlyakov, V. M., Legrand, M., Lipenkov, V. Y., Lorius, C., Pépin, L., Ritz, C., Saltzman, E., and Stievenard, M: Climate and atmospheric history of the past 420,000 years from the Vostok ice core, Antarctica, Nature, 399, 429–436, https://doi.org/10.1038/20859, 1999.

Pettit, L. R., Hart, M. B., Medina-Sánchez, A. N., Smart, C. W., Rodolfo-Metalpa, R., Hall-Spencer, J. M., and Prol-Ledesma, R. M.: Benthic foraminifera show some resilience to ocean acidification in the northern Gulf of California, Mexico, Mar. Pollut. Bull., 73(2), 452–462, https://doi.org/10.1016/j.marpolbul.2013.02.011, 2013.

Pettit, L. R., Smart, C. W., Hart, M. B., Milazzo, M., and Hall-Spencer, J. M.: Seaweed fails to prevent ocean acidification impact on foraminifera along a shallow-water CO_2 gradient. Ecol. Evol., 5(9), 1–10. https://doi.org/10.1002/ece3.1475, 2015.

Pierrot, D. E., Levis, E., and Wallace, D. W. R.: MS Excel Program Developed for CO_2 System Calculations. Oak Ridge, TN: U.S. Department of Energy: Carbon Dioxide Information Analysis Center, Oak Ridge National Laboratory, 2006.

Prazeres, M., Uthicke, S., and Pandolfi, J. M.: Ocean acidification induces biochemical and morphological changes in the calcification process of large benthic foraminifera, Proceedings B, 282, 20142782, https://doi.org/10.1098/rspb.2014.2782, 2015.

Price, N. N., Martz, T. R., Brainard, R. E., and Smith, J. E.: Diel variability in seawater pH relates to calcification and benthic community structure on coral reefs, PLoS ONE, 7(8), e4384, https://doi.org/10.1371/journal.pone.0043843, 2012.

R Core Team: R: A language and environment for statistical computing. R Foundation for Statistical Computing, Vienna, Austria, https://www.R-project.org/, 2020.

Sariaslan, N., and Langer, M. R.: Atypical, high-diversity assemblages of foraminifera in a mangrove estuary from Northern Brazil, Biogeosciences, 18, 4073–4090, https://doi.org/10.5194/bg-2021-56, 2021.

Schiebel, R.: Planktic foraminiferal sedimentation and the marine calcite budget. Global Biogeochem. Cycles, 16, 4, 3-1–3-21. https://doi.org/10.1029/2001GB001459, 2002.

Schneider, C. A., Rasband, W. S., and Eliceiri, K. W.: Nih Image to ImageJ: 25 years of image analysis, Nature Methods, 9, 7, 671–675, https://doi.org/10.1038/nmeth.2089, 2012.

Stephenson, C. M., Hallock, P., and Kelmo, F.: Foraminiferal assemblage indices: A comparison of sediment and reef rubble samples from Conch Reef, Florida, USA, Ecol. Indic., 48, 1–7, https://doi.org/10.1016/j.ecolind.2014.07.004, 2015.

Stuhr, M., Cameron, L. P., Blank-Landeshammer, B., Reymond, C. E., Doo, S. S., Westphal, H., Sickmann, A., and Ries, J. B.: Divergent proteomic responses offer insights into resistant physiological responses of a reef-foraminifera to climate change scenarios, Oceans, 2, 281–314, https://doi.org/10.3390/oceans2020017, 2021.

Toyofuku, T., Matsuo, M. Y., De Nooijer, L. J., Nagai, Y., Kawada, S., Fujita, K., Reichart, G. J., Nomaki, H., Tsuchiya, M., Sakaguchi, H., and Kitazato, H. Proton pumping accompanies calcification in foraminifera, Nat. Commun., 8(1), 14145, https://doi.org/10.1038/ncomms14145, 2017.

Uppström, L. R.: The boron/chlorinity ratio of deep-sea water from the Pacific Ocean, deep sea research and oceanographic abstracts, 21, 161–162, 1974.

Uthicke, S., Momigliano, P., and Fabricius, K. E.: High risk of extinction of benthic foraminifera in this century due to ocean acidification, Sci. Rep., 3, 1769, 1–5, https://doi.org/10.1038/srep01769, 2013.

Wilson, B., and Wilson, J.I.: Shoreline foraminiferal thanatacoenoses around five eastern Caribbean islands and their environmental and biogeographic implications, Cont. Shelf Res., 31(7–8), 857–866, https://doi.org/10.1016/j.csr.2011.02.010, 2011.

Yamano, H., Miyajima, T., and Koike, I.: Importance of foraminifera for the formation and maintenance of a coral sand cay: Green Island, Australia, Coral reefs, 19, 51–58, https://doi.org/10.1007/s003380050226, 2000.